Peer-reviewed version available at Appl. Sci. 2019, 9, 5301; doi:10.3390/app9245301

Article

Hydrogen Evolution on Nano-Structured CuO/Pd Electrode: Raman Scattering Study

Jurga Juodkazytė [1]*, Kęstutis Juodkazis [1], Ieva Matulaitienė [1], Benjaminas Šebeka [1], Irena Savickaja [1], Armandas Balčytis [2,3], Yoshiaki Nishijima [3,4], Gediminas Niaura [1], Saulius Juodkazis [2,4,5]*

[1] Center for Physical Sciences and Technology, Saulėtekio ave. 3, LT-10257 Vilnius, Lithuania
[2] Nanotechnology facility, Swinburne University of Technology, John st., Hawthorn, 3122 Vic, Australia
[3] Department of Electrical and Computer Engineering, Graduate School of Engineering, Yokohama National University, 79-5 Tokiwadai, Hodogaya-ku, Yokohama 240-8501, Japan
[4] Institute of Advanced Sciences, Yokohama National University, 79-5 Tokiwadai, Hodogaya-ku, Yokohama 240-8501, Japan
[5] Melbourne Center for Nanofabrication, Australian National Fabrication Facility, Clayton 3168, Melbourne, Australia
* Correspondence:jurga.juodkazyte@ftmc.lt (JJ); sjuodkazis@swin.edu.au (SJ)

Abstract: In this study the processes taking place on the surfaces of nanostructurized Cu/CuO and Cu/CuO/Pd electrodes at different potential, E, values in the solutions of 0.1 M KOH in H_2O and D_2O (heavy water) were probed by the surface enhanced Raman spectroscopy (SERS) and analysis of electrochemical reactions occurring under experimental conditions is presented. Bands of the SERS spectra of Cu/CuO/Pd electrode observed in the range of E values from +0.3 V to 0 V (SHE) at 1328 - 1569 cm^{-1} are consistent with the existence of species which are adsorbed or weakly bound to the surface with the energy of interaction close to 15 - 21 kJ mol^{-1}. These bands can be attributed to the ad(ab)sorbed $(H_3O^+)_{ad}$, $(H_2^+)_{ab}$ and $(H_2^+)_{ad}$ ions as intermediates in reversible HER/HOR processes taking place on Cu/CuO/Pd electrode. There was no isotopic effect observed; this is consistent with a dipole nature of electron-ion pair formation of adsorbed $(H_3O^+)_{ad}$ and $(H_2^+)_{ad}$ or $(D_3O^+)_{ad}$ and $(D_2^+)_{ad}$. In accordance with literature data SERS bands at 125-146 cm^{-1} and $\sim 520 - 565$ cm^{-1} were assigned to Cu(I) and Cu(II) oxygen species. These findings corroborate the mechanism of cascading reduction of water.

Keywords: nanostructured CuO; Pd electrode; hydrogen evolution; SERS

1. Introduction: Thermodynamics of hydrogen evolution reaction

The mechanisms of electrochemical hydrogen evolution and oxidation reactions (HER and HOR) are becoming a topic of interest again as hydrogen is expected to become the environmentally friendly fuel of the future.

In the recent literature [1–9] the interpretations of the mechanism of these processes taking place on the surface of various platinum group electrodes are based on the concept of adsorbed hydrogen atoms - H_{ad} as intermediate. In ref. [1] it suggested that in the range of low potential values adsorbed H_{ad} atoms are formed through a dissociative adsorption of H_2 rather than discharge of H^+ ions.

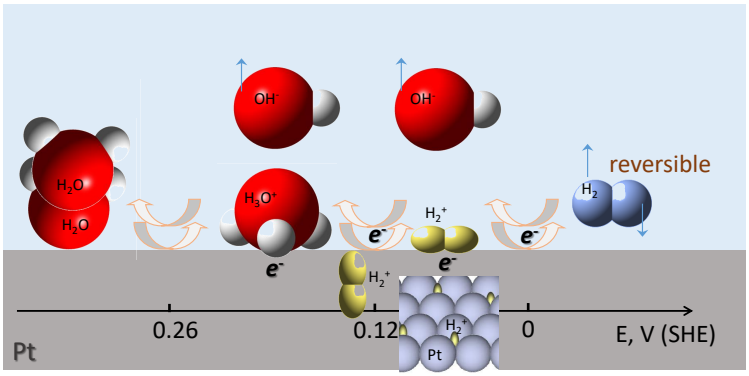

Figure 1. Mechanism of reversible stepwise water reduction/hydrogen oxidation via formation of ionic pairs at different potentials on Pt electrode [10]. This mechanism accounts *quantitatively* for the charge and mass changes on the electrode's surface.

It is defined by thermodynamics [11] that under the standard conditions, the processes of HER and HOR are described by the equation:

$$2H^+ + 2e^- \rightleftarrows H_2, \tag{1}$$

with the value of standard potential $E^0_{2H^+/H_2}$ = 0 V vs standard hydrogen electrode (SHE). However, it is also well known that the Volmer reaction:

$$H^+ + e^- \rightleftarrows H, \tag{2}$$

thermodynamically cannot proceed at $E = 0$ V (SHE), because the standard potential of the eq. (2) is E_{H^+/H^0} = -2.106 V [11]. As the hydrogen evolution reaction on Pt surface actually takes place at $E = 0$ V (SHE), it is assumed that the binding energy of H atoms in H_2 molecule is compensated by the energy of adsorption of H atoms leading to formation of H_{ad} on the electrode surface as intermediates of reaction 1. The energy of interaction between Pt electrode and H_{ad} is considered to be about 260 kJ mol^{-1} [8], i.e., slightly higher than $\Delta H_{chem} = \frac{1}{2} D_{H_2} \approx 226.8$ kJ mol^{-1} [12]; D is the binding energy of H_2. In accordance with the commonly accepted concept [1,7] formulated about 50 years ago [13–15], when the first H atom is adsorbed on the electrode surface in the form of H_{ad}, fully compensating half of the binding energy in H_2 molecule, the electrochemical discharge of the second H^+ ion and formation of H_2 at the equilibrium potential of 0 V (SHE) proceed without any hindrance. In other words, irreversible formation of H_2 molecule according to the summary equation 1 is possible with formation of the first adsorbed H_{ad} atom, i.e.:

$$H^+ + e^- \rightarrow H_{ad}, \tag{3}$$

followed by recombination according to Heyrovsky or Tafel paths as follows:

$$H_{ad} + H^+ + e^- \rightarrow H_2, \tag{4}$$

$$2H_{ad} \rightarrow H_2. \tag{5}$$

If the H_{ad} treated in various HER models would exist, thermodynamics requires to acknowledge that in the case of Pt, for instance, the energy of interaction between H_{ad} and the electrode surface should be equivalent to the energy of chemical bond, which can amount up to 260 kJ mol^{-1} [8]. The latter value,

however, is obviously incomparable with those corresponding to energy of adsorption. Moreover, it is well established [11] that hydrogen atom does not form any stable hydride-type compounds with many metals, including the Pt group ones. It can also be noted, that current peaks observed in cyclic voltammograms (CVs) of Pt electrode at $E > E^0_{2H^+/H_2}$ cannot be ascribed to the formation of monolayer of H_{ad} atoms weakly and strongly bonded to electrode surface, because, from the thermodynamic point of view, in the E range above 0 V (SHE) only oxidation of H_2 molecule can take place rather than underpotential discharge of H^+ to H_{ad}. In theory, the region of underpotential discharge of H^+ is confined to range of potentials between -2.1 V and 0 V.

In our previous study [10] based on the *quantitative* coulometric and micro-gravimetric analysis it was demonstrated that in the case of Pt electrode in the solution of 0.5 M H_2SO_4 the reversible electrochemical discharge of H_2O molecules proceeds according to the following reactions:

$$2H_2O + Q_{ad} \rightleftarrows (H_3O^+)_{ad} + OH^-, E^0 = 0.26 \text{ V (SHE)} \quad (6)$$

$$(H_3O^+)_{ad} + e^- \rightleftarrows (H_2{}^+)_{ad} + OH^-, E^0 = 0.12 \text{ V (SHE)} \quad (7)$$

$$(H_2{}^+)_{ad} + e^- \rightleftarrows H_2 + Q_{ad}, E^0 = 0 \text{ V (SHE)}. \quad (8)$$

Q_{ad} represents the adsorption charge which is drawn to the electrode surface to compensate the charge of adsorbed H_3O^+ or $H_2{}^+$ ions. This charge is approximately equivalent to one electron per one H_3O^+ or $H_2{}^+$ ion and it does not participate in the overall Faradaic HER as this term cancels upon summing of the eqs. (6)-(8).

At $E = 0$ V (SHE) steps (6) and (7) become fast and the overall process, which in the case of aqueous solutions is written as:

$$2H_2O + 2e^- \rightleftarrows H_2 + 2OH^- \quad (9)$$

corresponds to general HER/HOR eqn. (1). Equation (6) represents the process of H_2O dissociation and adsorption of H_3O^+ ion on the electrode surface and is reflected by the first reversible Langmuir-type adsorption peak in voltammograms of Pt electrode in sulfuric acid solution [10]. Reaction (7) is the reduction of $(H_3O^+)_{ad}$ leading to the formation of adsorbed $(H_2{}^+)_{ad}$ ion and corresponds to the second reversible Langmuir-type adsorption peak, whereas equation (8) represents the actual hydrogen evolution step on the Pt electrode, which determines the value of equilibrium potential $E^0_{2H^+/H_2}$ = 0 V (SHE) and the magnitude of exchange current i_0. As one can see from the eqs. (6) - (9), the role of intermediate in reversible H_2 evolution process is played by adsorbed hydrogen molecular ion $(H_2^+)_{ad}$. The existence of such ion has been corroborated in ref. [16] as well as a very high energy cost required for H^+ emission [17]. The binding energy between H^+ ion and H atom within H_2^+ is 255.7 kJ mol^{-1} [18], what is tantamount to the energy of adsorption indicated for H_{ad} atom and is sufficient for the reaction (7), which, in fact, is reduction of the first H^+ ion, to proceed. Thus there is no need to invoke H_{ad} atoms to explain the mechanism of reversible discharge of H_3O^+ ions. The energy of adsorption in the case of $(H_2^+)_{ad}$ intermediate is just 11.6 kJ mol^{-1}, as can be derived from the value of standard potential of eq. 7 according to $-\Delta G_{ads} = nFE^0$, whereas the ΔG_{ads} of $(H_3O^+)_{ad}$ (eq. 6) is 25.1 kJ mol^{-1} [10]. Such adsorbed intermediates are characteristic to Pt group metals. Maximum coverage of Pt electrode surface by either $(H_3O^+)_{ad}$ or $(H_2{}^+)_{ad}$ is just about 1/3 of the monolayer [10].

At $E^0 = 0$ V (SHE) the equilibrium surface concentration of $(H_2^+)_{ad}$ should be proportional to the bulk concentration of H_3O^+ and hydrogen pressure p_{H_2}, because otherwise the existence of reversible hydrogen electrode with $E = 0.000V - 0.059pH - 0.0295 \lg p_{H_2}$ would not be possible [11].

In the case of HOR, the surface electrochemical processes described by the eqs. (8),(7) and (6) proceed in a reverse manner. As the steric dimensions of molecular hydrogen ion are very small [10,19], absorption

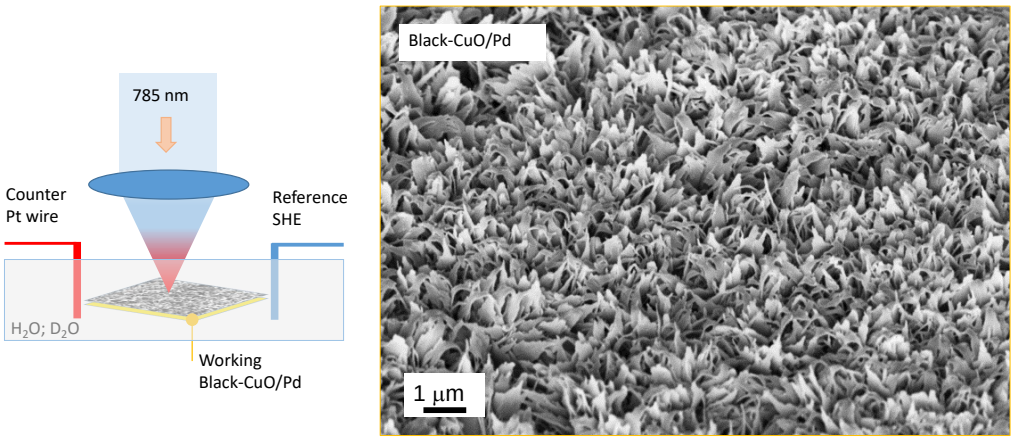

Figure 2. Setup for SERS measurements (in a back-scattering mode) in electrochemical cell with Pt wire as the counter electrode (CE), black-CuO or black-CuO/Pd as the working electrode (WE), and the reference electrode (RE) was the standard hydrogen electrode (SHE). SEM image of the WE black-CuO with a 200 nm Pd film.

of $(H_2^+)_{ad}$ during HER becomes possible and oxidation of the absorbed H_2^+ species is reflected by a minor anodic peak located between the two main ones [10].

Thus, as it is evident from the discussion above, hydrogen molecular ion H_2^+ unlocks understanding of the mechanism of the reversible hydrogen evolution process. In this novel concept $(H_2^+)_{ad}$ replaces H_{ad} as intermediate in HER and HOR and dissociative adsorption of H_2 is replaced by the stepwise dissociative ionization of hydrogen molecule according to eqs.(7) and (8) and was shown to account for mass and charge changes on the Pt electrode [10] (Fig. 1). Formally, H_3O^+ ion can be considered to contain one OH^- and two H^+ ions, which can be reduced to H_2 molecule via intermediate H_2^+ at E = 0 V (SHE) without violating the above described thermodynamic constrain and formation of H_{ad} on electrode surface. Validation of the cascading reduction mechanism (Fig. 1) by complimentary techniques, including optical, is highly required in order to get insights into efficient methods to control the efficiency of the overall HER process.

Surface enhanced Raman spectroscopy (SERS) is a sensitive method to elucidate the nature of intermediate compounds participating in hydrogen evolution and oxidation processes discussed above. In the present study, SERS was applied to investigate the HER and HOR processes on thin Pd layer sputtered on nano-structured copper-oxide substrate. Pd was chosen due to its well known ability to absorb significant amounts of hydrogen [20]. Reversible HER and HOR reactions on Pd surface are expected to follow the same route as on Pt electrode within E range from 0 V to 0.3 V (SHE), therefore the formation of $(H_3O^+)_{ad}$ and $(H_2^+)_{ad}$ ions should be anticipated. Correlation of the E-dependence of SERS response with electrochemical processes taking place on the electrode surface is presented and discussed in view of possible mechanism.

2. Experimental

Nanotextured surface of CuO was prepared via chemical oxidation method. As prepared and Pd coated electrodes were then used for spectroelectrochemical investigations using surface enhanced Raman spectroscopy (SERS) within various ranges of potential (Fig. 2).

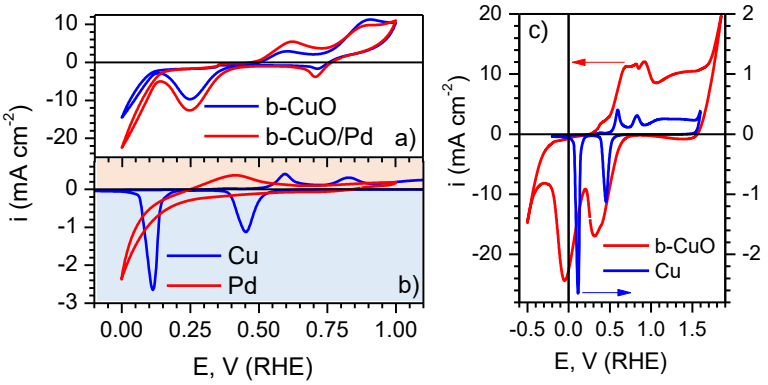

Figure 3. Cyclic voltammograms of: (a) black-CuO and black-CuO/Pd; (b) metallic Cu and Pd electrodes in 0.1 M KOH solution, potential scan rate 50 mV s^{-1}. The positive *E* limit of CV of metallic Cu in b) is at 1.6 V, just prior to the beginning of oxygen evolution reaction; the full range is not shown here for the sake of easier comparison with the curves in (a). (c) CVs within *E* range -0.5 - 1.85 V.

2.1. Samples for spectro-electrochemical measurements

Flat circular copper electrode of ca. 5 mm in diameter, press-fitted into a Teflon rod, was oxidized chemically as described in our previous paper [21] to produce SERS-active nanostructured Cu(II) oxide layer, further in the text referred to as black-CuO because of its black appearance due to anti-reflective surface texture. Using synchrotron X-ray surface analysis we have confirmed that only CuO is present on the surface of black-CuO [21] prepared by the method used in this study.

Plasma-enhanced chemical vapour deposition (PECVD) equipment (Axxis, JKLesker Ltd.) was used to sputter ∼200-nm-thick layer of Pd onto nanotextured surface of black-CuO electrodes. The electrode was placed closer to the sputtering target at the position where the coating rate was approximately 5 times larger than on the standard sample plane (an entire electrode in a tall teflon mount was placed inside the coating chamber). The coating conditions corresponded to a 40-nm-thick layer of Pd on a flat sample. Effective thickness of the coating was smaller than 40 nm due to an approximately 200 times larger surface area of the black-CuO as compared with the initial Cu substrate [22].

2.2. Electrochemical measurements

Electrochemical investigations were performed using potentiostat/galvanostat AUTOLAB 302. Three-electrode cell was employed to record voltammetric response of black-CuO, black-CuO/Pd samples, pure Pd and pure Cu (99.9%) samples, which were used as working electrodes. Pt plate (1 cm^2) and reference hydrogen electrode (RHE) in working solution served counter and reference electrodes, respectively. All potential values reported below refer to this reference electrode unless noted otherwise. Current density values in the text are normalized with respect to the geometric area of electrode. Solution of 0.1 M KOH was chosen for experiments in order to ensure the chemical stability of black-CuO substrate.

2.3. SERS measurements

Near-infrared Raman spectra were recorded using Echelle type spectrometer RamanFlex 400 (PerkinElmer, Inc.) equipped with thermoelectrically cooled (−50°C) CCD camera and fiber-optic cable for excitation and collection of the Raman spectra. The 785-nm beam of the diode laser was used as the excitation source. The 180° scattering geometry was employed. The laser power at the sample was restricted to 30 mW for SERS studies and the beam was focused to a 200 μm diameter spot on the electrode.

The integration time was 10 s. Polarisation of the light incident normally onto the electrode was linear while the polarization of the detected signal was not discriminated in polarisation.

Each spectrum was recorded by accumulation of 30 or 50 scans yielding the total integration times of 300 and 500 s. Spectro-electrochemical measurements were carried out in a cylinder-shaped three electrode moving cell, arranged with a nano-textured black-CuO or black-CuO/Pd as a working electrode (WE), platinum wire as a counter electrode (CE), and a RHE reference electrode (RE). The potential of the working electrode was changed stepwise, starting from the open-circuit potential (0.7 V) and going towards more negative E values to 0 V and -0.5 V for the black-CuO/Pd and black-CuO, respectively. During the experiment, solution was continuously bubbled by pure N_2 gas flow to remove dissolved oxygen. The WE was placed at approximately 3 mm distance from the cell window. In order to reduce photo and thermal effects, the cell together with the electrodes was moved linearly with respect to the laser beam with the rate of about 15-25 mm/s [23,24]. The Raman frequencies were calibrated using the polystyrene standard (ASTM E 1840) spectrum. Intensities were calibrated by NIST intensity standard (SRM 2241). Experiments were also carried out in heavy water D_2O to distinguish ionic hydrogen species by a Raman shift which is mass dependent; the D_2O related peaks appear at smaller wavenumbers in Raman scattering [25].

3. Results and Discussion

3.1. Voltammetric characterization

Figure 3a shows cyclic voltammograms of black-CuO and black-CuO/Pd electrodes recorded in 0.1 M KOH solution within E range between 0 and 1.0 V. The shape of both curves is essentially the same and the nature of the processes reflected by the voltammetric peaks can be easier understood when compared with the responses of pure metallic Pd and Cu electrodes presented in Fig. 3b. Anodic part of the cycles ($i > 0$) in Fig. 3a displays two peaks at 0.5 - 0.7 V and 0.75 - 1.0 V the position of which corresponds to the thermodynamic potential ranges of Cu_2O and CuO formation, respectively [11]. Such ascription of the peaks is supported by the fact that their positions coincide with those of anodic peaks observed in the voltammogram of pure Cu electrode in Fig. 3b. In the cathodic range of the CVs ($i < 0$), two peaks are observed as well (Fig. 3a). The first minor one at $E = 0.7$ V is situated in the range where reduction of CuO to Cu_2O is thermodynamically possible, however the amount of charge is very low. This peak could be ascribed to the reversible reduction of oxide species formed on the electrode surface in the preceding positive-going scan, whereas the main mass of nanostructured CuO, formed by means of chemical oxidation of Cu surface, is most likely reduced to Cu_2O in the range of second cathodic peak within 0.4 - 0.15 V. The latter peak is shifted towards more negative E values as compared with the first cathodic peak corresponding to transition CuO/Cu_2O in the case of pure Cu electrode in Fig. 3b. This means that reduction proceeds at an overpotential, which could be associated with the thickness of oxide layer on black-CuO electrode (it is noteworthy that current density values in Fig. 3a are tenfold compared to those in Fig. 3b). Reduction of Cu_2O to metallic Cu on black-CuO electrode proceeds at $E < 0.1$ V (Fig. 3a). In the case of Cu electrode, the sharp peak of Cu_2O reduction is between 0.2 V and 0 V (Fig. 3b). The comparison of CVs of black-CuO and Cu electrodes within wide range of potentials, i.e. -0.5 V - 1.85 V, encompassing the whole E window between O_2 and H_2 evolution reactions, is shown in Fig. 3c. One can see from the voltammogram of black-CuO in Fig. 3c that complete reduction of Cu_2O is achieved at the potentials as negative as -0.3 V. The voltammetric response of Pd in alkaline medium shown in Fig. 3b helps to identify the ranges of potential where one could expect to observe the influence of palladium in the CV of black-CuO/Pd electrode. The increase in cathodic current at $E < 0.3$ V on Pd electrode corresponds to HER, whereas anodic peak within 0.3 - 0.5 V is related to H_2 oxidation and desorption

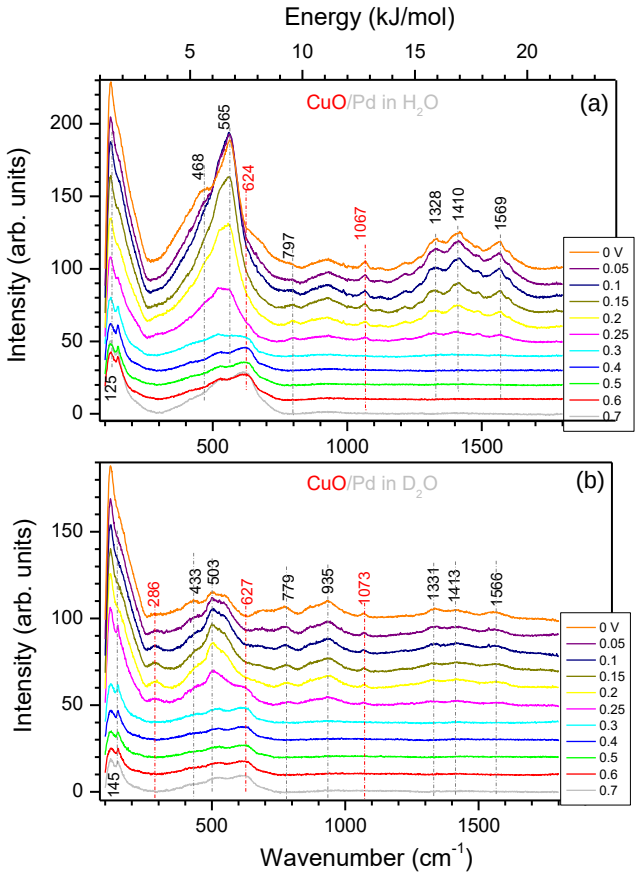

Figure 4. Dependence of the SERS spectra from black-CuO/Pd electrode upon the potential in 0.1 M KOH solution in water H_2O (a) and heavy water D_2O (b). Measurement conditions: laser excitation 785 nm; laser power at the sample 30 mW; integration time 300 s. Experiment was carried out under N_2 flow. The same electrode was used in both experiments. Spectral positions of the characteristic peaks are shown on vertical markers; red color markers denote CuO related bands. The main peak at 565 cm^{-1} in (a) corresponds to 70.1 meV energy or 6.76 kJ mol^{-1} (see, the upper horizontal axis).

processes. One can observe higher cathodic and anodic currents in the E ranges described above on black-CuO/Pd electrode as compared to Pd-free black-CuO sample Fig. 3a, however the assignment of these differences to influence of Pd is ambiguous. Most likely, the effect of Pd on black-CuO cannot be discerned in cyclic voltammograms, because Pd layer deposited by magnetron sputtering is very thin compared to the nanostructured CuO formed by chemical oxidation of Cu substrate. The influence of Pd on SERS response of black-CuO samples was significantly more obvious as described further.

3.2. Spectro-electrochemical measurements

Spectra of black-CuO/Pd and black-CuO electrodes recorded in 0.1 M KOH solution in normal and heavy water at fixed E values are shown in Figs. 4 and 5, respectively. From the viewpoint of HER, the main difference between Pd and Cu electrodes is that on palladium surface this process is reversible and takes place at $E = 0$ V (SHE), while in the case of copper hydrogen evolution reaction is irreversible and proceeds at an overvoltage of about 0.5 V [13], therefore more negative E range was chosen for investigations. It is evident from comparison of Figs. 4 and 5, that the intensity of spectra in the case of Pd-coated black-CuO electrode is about 10 times less. This, most likely, should be attributed to blocking of

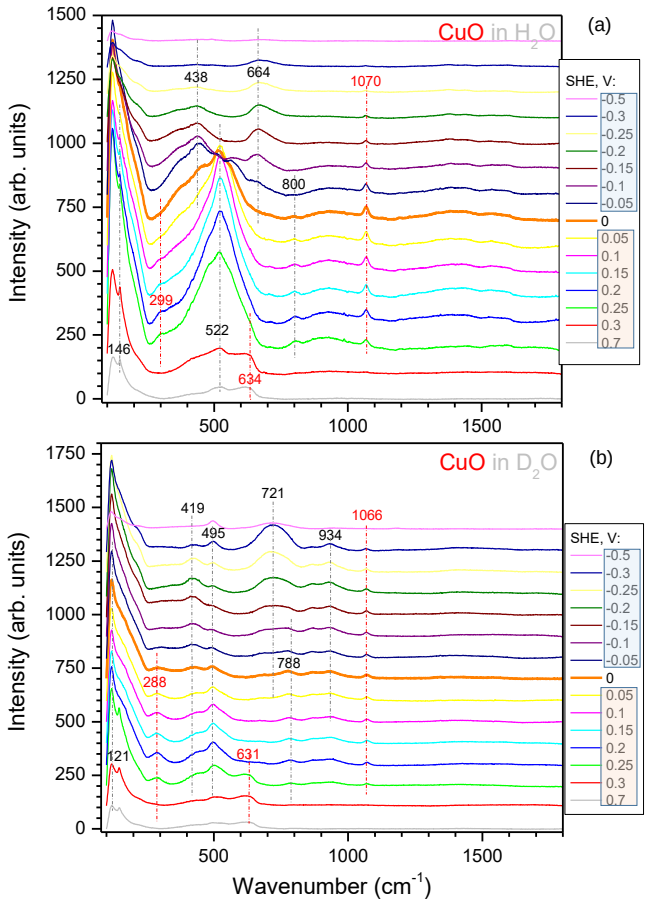

Figure 5. Dependence of the SERS spectra from black-CuO electrode upon the potential in 0.1M KOH solution in water H_2O (a) and heavy water D_2O (b). Measurement conditions: laser excitation 785 nm; laser power at the sample 30 mW; integration time 300 s. Experiment was carried out under N_2 flow. Spectral positions of the characteristic peaks are shown with vertical markers; red color markers denote CuO related bands.

the black-CuO surface by Pd, rather than decrease in electrode surface area, because evaporated $\sim$ 200 nm thick Pd layer cannot significantly reduce the true surface area of the electrode as we have found in earlier SERS studies [21].

All spectra in Figs. 4 and 5 can be conditionally divided into several regions. With respect to wavenumbers, one can make a distinction between the range at 100 - 800 cm^{-1}, where the most intensive bands are observed, and the other one at 800 - 1800 cm^{-1} with less intensive spectral features. From the viewpoint of electrode potential values, there is a clear distinction between the spectra recorded within 0.7 - 0.3 V, i.e. in the oxide region, and those obtained at $E < 0.3$ V, i.e. in the region of oxide reduction and hydrogen evolution reactions. The most prominent bands, which appear in all the spectra at 100 - 300 cm^{-1} and 400 and 600 cm^{-1} at the potentials just below 0.3 V and intensify as the electrode potential turns more negative should be assigned to cuprous oxide Cu_2O, which is produced by means of electrochemical reduction of CuO, as reflected by cathodic reduction peak within 0.15 - 0.4 V (Fig. 3a). At more negative potentials reduction of Cu_2O to Cu proceeds and this is the reason why the intensity of the bands indicated decreases significantly (see spectra at $E < 0.1$ V in Fig. 5a). The assignments of the CuO and Cu_2O bands

of the nanotextured surface was made following the earlier study of electrodes prepared by the same method [26] as well as literature data [27–32] and are summarized in Table A1, see the Supplement. The reason why the bands attributable to Cu_2O are less prominent in the spectra recorded in the solution of 0.1 M KOH in heavy water is, most likely, related to the fact that, that these spectra were collected after the experiments in normal water, during which the majority of CuO phase on black-CuO substrate was reduced.

The presence of Pd layer on black-CuO surface gives rise to the occurrence of distinct bands at 1328, 1410 and 1569 cm^{-1} observed in SERS spectra measured in the E range between 0.3 V and 0 V (RHE) (Fig. 4). Presuming that these bands correspond to the energy of adsorptive interaction between the particle and electrode surface, in the case of reversible HER they could be assigned to the adsorption of ionic intermediates $(H_2)^+_{ad}$, $(H_2)^+_{ab}$ $(H_3O^+)_{ad}$ on Pd surface with an energy of 15 - 21 kJ mol^{-1}. Such energy corresponds to Langmuir type adsorption process. Moreover the above indicated values correspond to the energy of H_2^+ and H_3O^+ adsorption on Pt electrode, i.e. 12 - 26 kJ mol^{-1} as determined from electrochemical data [10].

It is interesting to note that in the studies [33–36], devoted to IR spectroscopic investigations of HER/HOR processes on Pt electrode in 0.5 M H_2SO_4, it is presumed that adsorption of $(H_3O^+)_{ad}$ is reflected by band at 1100 cm^{-1}, whereas band within 2080 - 2095 cm^{-1} is assigned to discharging particle, which is H_{OPD} - overpotential deposited H atom. In terms of energy of interaction between the particle and the surface this would correspond to 14 - 26 kJ mol^{-1}.

Direct comparison of Raman spectra of the CuO electrode with and without Pd are replotted in Sec. 4 Figs. S1 and S2 for H_2O and D_2O, respectively, at the potential range of 0.3-0 V preceding to HER. A Pd deposition resulted in suppression of the most prominent Raman bands related to CuO, however, there was almost no effect at the spectral window of 1700-1300 cm^{-1}. Especially for the HER at 0 V in H_2O, there was almost no decrease in Raman intensity.

3.3. Isotopic effect in SERS

Comparison of spectra collected in the solutions of normal and heavy water (Fig. 4a vs 4b and Fig. 5a vs 5b) did not reveal clear isotopic effect in vibrational spectra of ions or molecules. In the case of bands attributed to Cu(I) and Cu(II) oxides such result is logical as their origin is not dependent on the solvent. This is also the case for weak ionic adsorption of $(H_2)^+_{ad}$, $(D_2)^+_{ad}$, $(H_3O^+)_{ad}$ and $(D_3O^+)_{ad}$ on Pt or Pd electrode surface: replacing water with heavy water does not effect the charge of the adsorbing particle and, consequently, the energy of its interaction with the surface as elaborated further.

In theory, the difference in vibrational bands between H_2O and D_2O is defined by a change in the reduced mass of the atoms involved $\mu_{xx} = m_x m_x/(m_x + m_x)$ where m_x denotes the mass of H or D atoms. The expected shift of the vibrational frequency due to H substitution by D can be estimated from $\nu_{XD} = \nu_{XH}\sqrt{\mu_{XH}/\mu_{XD}}$; one finds $\nu_{DD} = \nu_{HH}\sqrt{\mu_{HH}/\mu_{DD}}$. Hence, the bands related to the D_2O will be at smaller wavenumbers as compared to those in H_2O, correspondingly at $\sqrt{\mu_{HH}/\mu_{DD}} = 70.74\%$ of the energy (wavenumber). Such significant isotopic effect is expected for the interatomic bond in H_2 or D_2 molecules. A certain isotopic effect could be expected if evolution of D_2 went through the formation of stable chemisorbed compound between D_{ad} and the electrode surface, whereas for the weakly adsorbed surface species the energy of adsorption of charged $(H_2^+)_{ad}$ and $(D_2^+)_{ad}$ particles in the potential range investigated is, most likely, almost the same, due to electrostatic nature of the interaction (a spring constant k of a harmonic oscillator is the same considering mechanical analogy). Due to the same charges and similar size of the adsorbing particles, the isotopic effect was not pronounced.

From the viewpoint of energetic considerations, SERS spectra reflect the energy of interaction between a particle and electrode surface defined by potential constant k and the reduced mass μ. The oscillator

frequency $\omega = \sqrt{k/\mu}$ for small k and μ (in the electron-ion pair, the electron mass dominates μ), a small change in vibration energy quanta $\hbar\omega$ is expected between H and D as observed in the experiment. Since dipole absorption is not Raman active (a negligible polarisability), it is expected that formation of electron-ion pairs with strong dipole interaction at the interface investigated here were difficult to identify by spectral shift in Raman spectroscopy. Appearance of Raman bands at the 15-21 kJ/mol or 1320 - 1570 cm^{-1} wavenumbers window leading to hydrogen evolution are consistent with the cascading reduction mechanism (Fig. 1).

4. Conclusions

The reactions taking place on the surfaces of nanostructurized Cu/CuO and Cu/CuO/Pd electrodes at different potential, E, values in the solutions of 0.1 M KOH in normal and heavy water were studied using the surface enhanced Raman spectroscopy technique. The following conclusions can be drawn:

1. A clear correlation between the SERS spectra and potential-governed surface state of the electrodes investigated was determined. However, due to a dipole nature of the electron-ion pair, the Raman signatures were expected to be weak.
2. The SERS spectra measured at controlled electrode potential of black-CuO/Pd electrode are consistent with the existence of weakly adsorbed $(H_3O^+)_{ad}$ and $(H_2^+)_{ad}$ ions as intermediate in the reversible HER/HOR processes in the region of E potentials from +0.3 V to 0 V (SHE) and wavenumber region from 1320 to 1570 cm^{-1}. Because of the low energy of interaction with surface, i.e. 15 - 21 kJ mol^{-1}, these adsorption compounds cannot be treated as Pd hydrides.
3. It is shown that SERS bands observed at wavenumbers 125 - 146 cm^{-1} and 520 - 565 cm^{-1} in 0.1 M KOH solution in the range of the potentials between 0.7 and -0.5 V (RHE) correspond to Cu(I) and Cu(II) oxygen species.

Author Contributions: Author contributions: conceptualization, J.J. and K.J.; methodology, G.N. and I.M.; SERS experiments, G.N. and I.M.; electrochemical experiments, B.Š and I.S.; preparation of electrodes, A.B; writing—original draft, J.J.; visualization, S.J.; discussion and data analysis J.J., K.J., Y.N., G.N., S.J.; all authors contributed to the final editing of the manuscript.

Funding: This research was partially funded by ARC grant number DP190103284.

Conflicts of Interest: The authors declare no conflict of interest.

References

1. Mercer, M.P.; Hoster, H.E. Electrochemical Kinetics: a Surface Sciene-Supported Picture of Hydrogen Electrochemistry on Ru(0001) and Pt/Ru(0001). *Electrocatalysis* **2017**, *8*, 518–529.
2. Fang, Y.H.; Wei, G.F.; Liu, Z.P. Catalytic Role of Minority Species and Minority Sites for Electrochemical Hydrogen Evolution on Metals: Surface Charging, Coverage, and Tafel Kinetics. *J. Phys. Chem. C* **2013**, *117*, 7669–7680.
3. Shinagawa, T.; Garcia-Esparza, A.; Takanabe, K. Insight on Tafel slopes from a microkinetic analysis of aqueous electrocatalysis for energy conversion. *Sci. Reports* **2015**, *5*, 13801.
4. Li, J.; Ghoshal, S.; Bates, M.K.; Miller, T.E.; Davies, V.; Stavitski, E.; Attenkofer, K.; Mukerjee, S.; Ma, Z.F.; Jia, Q. Experimental Proof of the Bifunctional Mechanism for the Hydrogen Oxidation in Alkaline Media. *Angewandte Chemie Int. Ed.* **2017**, *56*, 15594–15598.
5. He, Z.D.; Wei, J.; Chen, Y.X.; Santos, E.; Schmickler, W. Hydrogen evolution at Pt(111) - activation energy, frequency factor and hydrogen repulsion. *Electrochimica Acta* **2017**, *255*, 391 – 395.
6. Angerstein-Kozlowska, H. *Comprehensive Treaties of Electrochemistry*; Vol. 9, Plenum Press, New York, 1984.
7. Conway, B.E.; Tilak, B.V. Interfacial processes involving electrocatalytic evolution and oxidation of H_2, and the role of chemisorbed H. *Electrochimica Acta* **2002**, *47*, 3571–3594.

8. Jerkiewicz, G. Hydrogen sorption AT/IN electrodes. *Prog. Surf. Sci.* **1998**, *57*, 137–186.
9. Lasia, A. On the mechanism of the hydrogen absorption reaction. *J. Electroanal. Chem.* **2006**, *593*, 159–166.
10. Juodkazis, K.; Juodkazytė, J.; Šebeka, B.; Juodkazis, S. Reversible hydrogen evolution and oxidation on Pt electrode mediated by molecular ion. *Appl. Surf. Sci.* **2014**, *290*, 13–17.
11. Pourbaix, M. *Atlas d'équilibres électrochimiques*; Gauthier-Villars, Paris, 1963.
12. Emsley, J. *The Elements*, 2 ed.; Clarendon Press, Oxford, 1991.
13. Vetter, K.J. *Elektrochemische kinetik*; Springer-Verlag, Berlin-Gottingen, 1961.
14. Will, F.G.; Knorr, C.A. Untersuchung von Adsorptionserscheinungen an Rhodium, Iridium, Palladium und Gold mit der potentiostatischen Dreieckmethode. *Zeitschrift für Electrochemie* **1960**, *64*, 270–275.
15. Biegler, T.; Rand, D.A.J.; Woods, R. Limiting oxygen coverage on platinized platinum; Relevance to determination of real platinum area by hydrogen adsorption. *J. Electroanal. Chem.* **1971**, *29*, 269–277.
16. Rajgara, F.A.; Dharmadhikari, A.K.; Mathur, D.; Safvan, C.P. Strong fields induce ultrafast rearrangement of H atoms in H2O. *J. Chem. Phys.* **2009**, *130*, 231104.
17. Xie, X.; Roither, S.; Larimian, S.; Erattupuzha, S.; Zhang, L.; He, F.; Baltuška, A. Zero-energy proton dissociation of H through stimulated Raman scattering. *arXiv:1901.10743*.
18. Rabinovich, V.A.; Khavin, Z.Y. *Kratkiy khimicheskiy spravochnik*; Khimiya, Leningrad, 1977.
19. Juodkazis, K.; Juodkazytė, J.; Grigucevičienė, A.; Juodkazis, S. Hydrogen species within the metals: role of molecular hydrogen ion H_2^+. *Appl. Surf. Sci.* **2011**, *258*, 743–747.
20. Nishijima, Y.; Shimizu, S.; Kurihara, K.; Hashimoto, Y.; Takahashi, H.; Balcytis, A.; Seniutinas, G.; Okazaki, S.; Juodkazyte, J.; Iwasa, T.; Taketsugu, T.; Tominaga, Y.; Juodkazis, S. Optical readout of hydrogen storage in films of Au and Pd. *Optics Express* **2017**, *25*, 24081–24092.
21. Balčytis, A.; Ryu, M.; Seniutinas, G.; Juodkazytė, J.; Cowie, B.C.C.; Stoddart, P.R.; Morikawa, J.; Juodkazis, S. Black-CuO: Surface-enhanced Raman scattering and infrared properties. *Nanoscale* **2015**, *7*, 18299–18304.
22. Juodkazytė, J.; Šebeka, B.; Savickaja, I.; Selskis, A.; Jasulaitienė, V.; Kalinauskas, P. Evaluation of electrochemically active surface area of photosensitive copper oxide nanostructures with extremely high surface roughness. *Electrochimica Acta* **2013**, *98*, 109 – 115.
23. G. Niaura, A. K. Gaigalas, V.L.V. Moving spectroelectrochemical cell for surface Raman spectroscopy. *J. Raman Spectrosc.* **1997**, *28*, 1009–1011.
24. Bulovas, A.; Dirvianskytė, N.; Talaikytė, Z.; Niaura, G.; Valentukonytė, S.; Butkus, E.; Razumas, V. Electrochemical and structural properties of self-assembled monolayers of 2-methyl-3-(?-mercaptoalkyl)-1,4-naphthoquinones on gold. *J. Electroanal. Chem.* **2006**, *591*, 175–188.
25. Savinova, E.; Zemlyanov, D.; Pettinger, B.; Scheybal, A.; Schlogl, R.; Doblhofer, K. On the mechanism of Ag(111) sub-monolayer oxidation: a combined electrochemical, in situ SERS and ex situ XPS study. *Electrochimica Acta* **2000**, *46*, 175 – 183.
26. J.Juodkazyte.; B.Šebeka.; I.Savickaja.; A.Jagminas.; V.Jasulaitiene.; A.Selskis.; J.Kovger.; P.Mack. Study on copper oxide stability in photoelectrochemical cell composed of nanostructured TiO_2 and Cu_xO electrodes. *Electrochimica Acta* **2014**, *137*, 363–371.
27. Niaura, G. Surface-enhanced Raman spectroscopic observation of two kinds of adsorbed OH- ions at copper electrode. *Electrochimica Acta* **2000**, *45*, 3507–3519.
28. Chan, H.Y.H.; Takoudis, C.G.; Weaver, M.J. Oxide Film Formation and Oxygen Adsorption on Copper in Aqueous Media As Probed by Surface-Enhanced Raman Spectroscopy. *J. Phys. Chem.* **1999**, *103 (2)*, 357–365.
29. Yu, P.; Shen, Y. Resonance Raman studies in Cu_2O. I. The phonon-assisted 1s yellow excitation absorption edge,. *Phys. Rev. B* **1975**, *12*, 1377.
30. Maji, S.; Mukherjee, N.; Mondal, A.; Adhikary, B.; Karmakar, B. Chemical synthe-sis of mosoporous CuO from a single precursor: structural, optical and electricproperties,. *J. Solid State Chem.* **2010**, *183*, 1900.
31. Wang, W.; Zhou, Q.; Fei, X.; He, Y.; Zhang, P.; Zhang, G.; Peng, L.; Xie, W. Synthe-sis of CuO nano- and micro-structures and their Raman spectroscopic studies,. *CrystEngComm* **2010**, *12*, 2232.
32. Debbichi, L.; de Lucas, M.M.; Pierson, J.; Krüger, P. Vibrational propertiesof CuO and Cu_4O_3 from first-principles calculations and Raman and infraredspectroscopy. *J. Phys. Chem. C* **2012**, *116*, 10232.

33. Masahashi Nakamura, Toshiki Kobayashi, N.H. Structural dependence of intermediate species for the hydrogen evolution reaction on single crystal electrodes of Pt. *Surface Sci.* **2011**, *605*, 1462–1465.
34. Kunimatsu, K.; Senzaki, T.; Tsushima, M.; Osawa, M. A combined surface-enhanced infrared and electrochemical kinetics study of hydrogen adsorption and evolution on a Pt electrode. *Chem. Phys. Lett.* **2005**, *401*, 451–454.
35. Kunimatsu, K.; Uchida, H.; Osawa, M.; Watanabe, M. In situ infrared spectroscopic and electrochemical study of hydrogen electro-oxidation on Pt electrode in sulfuric acid. *J. Electroanalytical Chem.* **2006**, *587*, 299–307.
36. Kunimatsu, K.; Senzaki, T.; Samjeske, G.; Tsushima, M.; Osawa, M. Hydrogen adsorption and hydrogen evolution reaction on a polycrystalline Pt electrode studied by surface-enhanced infrared absorption spectroscopy. *Electrochimica Acta* **2007**, *52*, 5715–5724.

Supplement

Various scenarios of HER: $2H_2O + 2e^- \rightarrow H_2 + 2OH^-$				
	Reversible	Irreversible	Hydride route	Oxide route
Electrodes	Pt group metals *(e. g. Pt, Pd, Rh, Ir)*	Various metals *(e. g. Pt, Pd, Au, Ag, Co, Ni, Fe, Cu and other metals not forming hydrides at E ≥ -1.2 V)*	Metals and other elements forming surface hydrides *(e. g. Si, Bi, Sb, Pb, Sn)*	Metals and other elements forming multivalent oxides *(e. g. Re, W, Mo, Nb, Ti, Ta)*
Reactions	$2H_2O \Leftrightarrow (H_3O^+)_{ad} + OH^-$ $(H_3O^+)_{ad} + e^- \Leftrightarrow (H_2^+)_{ad} + OH^-$ $(H_2^+)_{ad} + e^- \Leftrightarrow H_2$	$2H_2O \Leftrightarrow (H_3O^+)_{ad} + OH^-$ $(H_3O^+)_{ad} + 2e^- \rightarrow H_2 + OH^-$	$Me + H_2O + e^- \rightarrow MeH_{hydr} + OH^-$ $MeH_{hydr} + H_2O + e^- \rightarrow H_2 + OH^- + Me$ H_{hydr} represents H atom chemisorbed on metal or other element surface	Electrochemical reduction of oxide to lower oxide Chemical reaction between lower oxide and H_2O with formation of H_2
Intermediate	$(H_2^+)_{ad}$	$(H_3O^+)_{ad}$	MeH_{hydr}	Oxide of intermediate valence
Features	$E = E^0$ $i_0 \approx 0.1$ mA cm^{-2} $dE/dlgi = RT/F$ $i << i_0$ Formation of $(H_3O^+)_{ad}$ and $(H_2^+)_{ad}$ adsorption layers at $E > E^0$	$E < E^0$ $dE/dlgi = 2RT/F$ $i >> i_0$ value of overpotential, η, depends on the conditions which determine access of H_3O^+ ion to electrode surface	$E < E^0$ various values of $dE/dlgi$ value of η depends on the energy of chemical bond in Me-H_{hydr}	$E < E^0$ various values of $dE/dlgi$ value of η depends on the formation of the oxide of intermediate valence

Suppl. Fig. A1. Scenarios of HER on different materials.

Comparison of Raman spectra of Pd coated and uncoated black-CuO electrodes in H_2O (Fig. A2) and D_2O (Fig. A3), respectively. Sputtered film of Pd has reduced the major CuO-related bands however, at the 0 V where HER is taking places there was only small change observed (Fig. A2). It is noteworthy that the absorbance of heavy water is by order of magnitude smaller at the vis-IR spectral range used for excitation of Raman scattering. This is related to the smaller Raman intensity in the case of heavy water experiments.

Appendix .1 Different Hydrogen evolution scenarios

In addition to the above presented mechanism of H_3O^+ discharge, there are many other mechanisms of hydrogen evolution reaction, which depend on the specific conditions under which reaction occurs. Various possible scenarios of HER are summarized in Fig. A1. When H_3O^+ ion present in the solution bulk is reduced on the electrode surface at $i >> i_0$, irreversible scenario occurs, which should also proceed via the stage of H_2^+, but without the formation of the adsorption layer. The beginning of the irreversible process is also at 0 V (SHE).

When surface hydrides can form, direct reduction of H_2O molecules may occur (see the Hydride route in Fig. A1). An addition of a second H atom to form H_2 molecule is facile. It proceeds according to the Heyrovsky or Tafel path [11] at overpotential, η, the magnitude of which is determined by the energy of chemisorption of hydride species H_{hydr}. It is noteworthy that the concept of H_{ad} is not equivalent to that of H_{hydr}, because the former is understood as adsorption of H atom on the electrode surface with the energy of 260 kJ mol^{-1}, whereas in H_{hydr} hydrogen atom can be chemisorbed on the surface with considerably smaller energy in the E range from 0 V to -2.1 V (SHE). In this case the energy of discharge of the first H^+ ion is compensated by the energy of MeH_{hydr} formation and the overvoltage, η, i.e. $\Delta G_{\mathrm{hydr}} + e\eta \approx \frac{1}{2} D_{H_2} \approx 226.8$ kJ mol^{-1}.

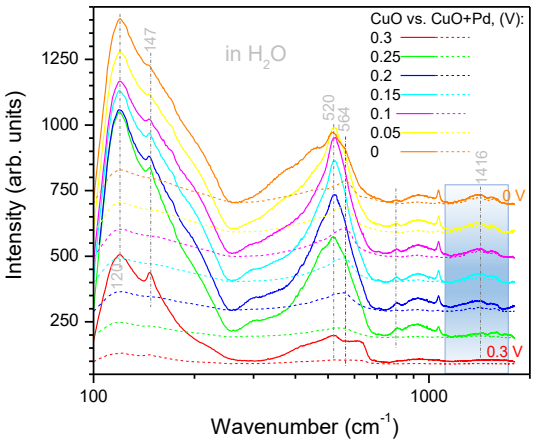

Suppl. Fig. A2. SERS in water. Comparison of CuO electrode with and without Pd coating. Note the logarithmic scale of the wavenumber axis. Shaded region marks spectral range where decrease of the Raman bands due to Pd was minimal. Note the logarithmic scale of the wavenumber axis.

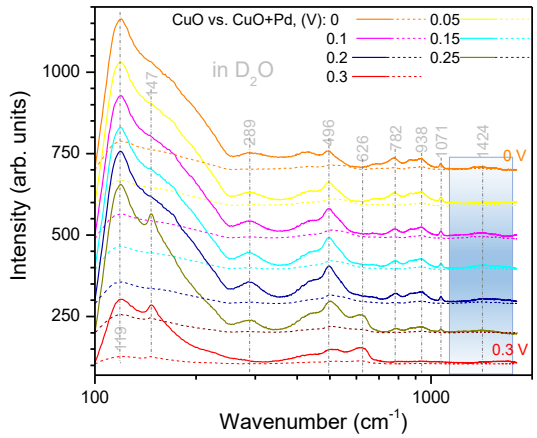

Suppl. Fig. A3. SERS in heavy water. Comparison of CuO electrode with and without Pd coating. Note the logarithmic scale of the wavenumber axis.

In the last case, referred to as the Oxide route in Table A1, when the electrode surface is covered with the oxide of intermediate valence, low values of η (e.g. on rhenium) are observed when O^{2-} ion is subtracted from H_2O molecule and H_2 is formed from two remaining H^+ ions with simultaneous transition of the oxide back to its former stable state. As obvious from the above discussion, there are different scenarios of HER and they should be analyzed specifically, taking into consideration possible intermediates forming on the electrode surface and the H_{ad} intermediate is neither realistic, nor universal.

Table A1. Band assignments.

Wavenumber [cm^{-1}]		
Black-CuO H_2O/D_2O	Black-CuO/Pd H_2O/D_2O	Assignment
–/121	125/–	CuO; this work
146/–	–/145	$Cu_2O\ \Gamma_{15}^{-(1)}$ [27,28,32]
299/288	–/ 286	CuO A_g [30–32]
438/419		Cu-OH (426 cm^{-1}[27,28])
	468/433	Cu-OH shifted;[27,28]
522/495	–/ 503	Cu_2O,Cu-OH Γ_{25}^{+} [27,28,32]
560/–	565/–	CuO_2 [27,28]
	624/627	CuO_2 [27,28]
634/631		$Cu_2O\Gamma_{15}^{-(2)}$
		623 [27], 640 [29], 645 cm^{-1} [32]
664/–		
–/721		
800/788	797/779	Cu-OH shifted [27,28]